Biomedicine & Pharmacotherapy 139 (2021) 111579

Contents lists available at ScienceDirect

Biomedicine & Pharmacotherapy

journal homepage: www.elsevier.com/locate/biopha

Original article

Supplementation with ribonucleotide-based ingredient (Ribodiet®) lessens oxidative stress, brain inflammation, and amyloid pathology in a murine model of Alzheimer

Anella Saviano [a,1], Gian Marco Casillo [a,1], Federica Raucci [a], Alessia Pernice [a], Cristina Santarcangelo [b], Marialuisa Piccolo [b], Maria Grazia Ferraro [b], Miriam Ciccone [c], Alessandro Sgherbini [d], Nadia Pedretti [d], Daniele Bonvicini [d], Carlo Irace [b], Maria Daglia [b], Nicola Mascolo [a,*], Francesco Maione [a,*]

[a] ImmunoPharmaLab, Department of Pharmacy, School of Medicine and Surgery, University of Naples Federico II, Via Domenico Montesano 49, 80131 Naples, Italy
[b] Department of Pharmacy, School of Medicine and Surgery, University of Naples Federico II, Via Domenico Montesano 49, 80131 Naples, Italy
[c] Department of Pharmacy, University of Salerno, Via Giovanni Paolo II 132, 84084 Fisciano, Salerno, Italy
[d] Prosol S.p.A., Via Carso, 99, 24040 Madone, Bergamo, Italy

ARTICLE INFO

Keywords:
Alzheimer's disease
Neuro-inflammation
Ribodiet®
Ribonucleotides
Iron metabolism

ABSTRACT

Alzheimer's disease (AD) is the most common type of dementia worldwide, characterized by the deposition of neurofibrillary tangles and amyloid-β (Aβ) peptides in the brain. Additionally, increasing evidence demonstrates that a neuroinflammatory state and oxidative stress, iron-dependent, play a crucial role in the onset and disease progression. Besides conventional therapies, the use of natural-based products represents a future medical option for AD treatment and/or prevention. We, therefore, evaluated the effects of a ribonucleotides-based ingredient (Ribodiet®) in a non-genetic mouse model of AD. To this aim, mice were injected intracerebroventricularly (i.c.v.) with $A\beta_{1-42}$ peptide (3 μg/3 μl) and after with Ribodiet® (0.1–10 mg/mouse) orally (p.o.) 3 times weekly for 21 days following the induction of experimental AD. The mnemonic and cognitive decline was then evaluated, and, successively, we have assessed *ex vivo* the modulation of different cyto-chemokines on mice brain homogenates. Finally, the level of GFAP, S100β, and iron-related metabolic proteins were monitored as markers of reactive gliosis, neuro-inflammation, and oxidative stress. Results indicate that Ribodiet® lessens oxidative stress, brain inflammation, and amyloid pathology *via* modulation of iron-related metabolic proteins paving the way for its rationale use for the treatment of AD and other age-related diseases.

1. Introduction

Alzheimer's disease (AD) is the most common type of dementia worldwide [1], clinically characterized by cognitive decline and behavioral alterations [2,3]. Pathologically, it presents accumulation of amyloid-β (Aβ) plaques, neuronal degeneration, glial activation, and a persistent neuro-inflammation due to the increased production of pro-inflammatory cytokines such as interleukin (IL)-1α, IL-16, IL-17, intercellular adhesion molecule-1 (ICAM-1), and chemokine CXC ligand (CXCL)-12, mainly up-regulated in the pre-frontal cortex and hippocampus [4,5].

Recent evidence also highlights the pathological role of iron

Abbreviations: AD, Alzheimer's disease; Aβ, amyloid-β; C5a, complement component 5a; CNS, central nervous system; CXCL, CXC ligand; ELISA, enzyme-linked immunosorbent assays; Fe^{2+}, ferrous iron; FGF-2, fibroblast growth factor-2; Fer, ferritin; GFAP, glial fibrillary acidic protein; ICAM-1, intercellular adhesion molecule-1; IL, interleukin; i.c.v., intracerebroventricular; IRP-1, iron regulatory protein-1; KC, keratinocyte-derived cytokine; MIP, macrophage inflammatory protein; NOR, novel object recognition; p.o., orally; ROS, reactive oxygen species; S100β, calcium-binding protein β; SDF-1, Stromal derived factor-1; Tf, transferrin; TfR-1, transferrin Receptor-1; TGF-β, transforming growth factor-beta; TIMP, tissue inhibitors of metalloproteinase; TREM-1, triggering receptor expressed on myeloid cells-1.

* Corresponding authors.
E-mail addresses: nicola.mascolo@unina.it (N. Mascolo), francesco.maione@unina.it (F. Maione).
[1] These authors share first co-authorship.

https://doi.org/10.1016/j.biopha.2021.111579
Received 22 February 2021; Received in revised form 29 March 2021; Accepted 31 March 2021
Available online 10 April 2021

metabolism dysregulation in the onset and AD progression [6,7]. Particularly, ferrous iron (Fe^{2+}), a metal required for normal cellular metabolism, acts as a catalyst in the Fenton's reaction that generates free radical species, including hydroxyl radicals (•OH) that can exacerbate the oxidative stress related to AD onset [8–10]. In support of these hypotheses, high levels of iron content and related reactive oxygen species (ROS) have been detected in the AD brain [11]. Accordingly, the current knowledge suggested that, in the brain, the iron balance depends on the normal expression of proteins that control its uptake (transferrin Receptor-1; TfR-1), release, storage (ferritin; Fer), and transport (transferrin; Tf). Ferritin is considered the endpoint of iron metabolism due to its involvement in removing and storing iron excess to reduce cellular injury and oxidative stress [12]. Moreover, it has been reported that perturbation of iron homeostasis in the brain is reflected peripherally by haematological values [13,14]. Accordingly, Faux and coll. demonstrated that AD patients had significantly lower systemic haemoglobin levels with a pathological change of transferrin-haemoglobin ratio, as a consequent alteration of iron transportation to bone marrow [15].

On the other hand, elevated oxidative stress (particularly iron-mediated) has been shown to impair physiological cellular bioenergetics and intensify by depleting nucleosides and nucleotides that have a significant role in cognitive and motor functions [16,17]. In this context, Alonso-Andrèes and coll. [18] reported that during the early stages of AD occurs an alteration of purines and pyrimidines metabolic pathways, nitrogenous bases involved in the core reaction of nucleosides, nucleotides, DNA, and RNA synthesis [19]. Accordingly, in several studies have been reported the positive neurotrophic effects exerted by nucleotides, especially ribonucleotides, in hippocampal neurons and glial cells [20], where these components seem to induce the release of those endogenous protective factors such as transforming growth factor-beta (TGF-β) and fibroblast growth factor-2 (FGF-2) [21] that interrupt amyloidogenic pathways promoted by AD-related oxidative stress [22].

Given the notable contribution of neuro-inflammation and iron metabolism in AD and the stringent involvement of nucleosides and nucleotides on neuronal functions, we decided to examine whether a ribonucleotides-based ingredient could ameliorate Aβ-induced neuroinflammation and oxidative stress.

2. Materials and methods

2.1. Reagents

Ribodiet® (batch number #D3/058420) was supplied and certificated by PROSOL S.p.A. (Certificate of analysis in Supplementary Fig. 1). This natural product, extracted from *Kluyvermomyces Fragilis* (ratio quantity of the genuine initial preparation/final product 15:1 kg), with a gentle, standardized, and highly controlled process, solvent-free, is a source of nucleotides (expressed as heptahydrate, > 40% 7 H_2O), nucleosides, oligonucleotides, ribonucleic acids fragments, amino acids, minerals, and group B vitamins (Table 1). The starting raw material, filtered by microfiltration (by 0.45 μm membranes) to separate suspended particles from the process liquid, was subjected to a first dilution by adding osmotic water until a pH value of 5.5. The mass thus obtained was subjected to a heat treatment step, at a temperature between 90 °C and 100 °C for 20–30 min, followed by a cooling process by adding water in quantity sufficient to lower the temperature to 70 °C. The conditions thus obtained (70 °C and pH between 5.3 and 5.5) are those considered optimal for the activity of the enzyme necessary to hydrolyze RNA. The obtained enzyme, dissolved in a separated container of 10–15 L, was then added into the reactor before a hydrolysis process of 10 h at 70 °C. Finally, the mass was subjected to a centrifugation step in a clarifying centrifuge and a subsequent concentration step under vacuum.

Full technical data sheet specification is reported in Supplementary Fig. 2. HPLC profile and standards methods (Supplementary Fig. 3) were conducted following ISO directives (78-2:1999) and EMA guidelines for herbal medicinal products [23].

Table 1
Schematic description of quali-quantitative Ribodiet® profile.

AA	Quantity	Unit of Measurement
Aspartic Ac. incl. Asparagine	1.4	g/100 g
Glutammico Ac. incl. Glutammine	2.1	g/100 g
Alanine	0.8	g/100 g
Arginine	0.7	g/100 g
Glycine	1.6	g/100 g
Leucine	0.7	g/100 g
Lysine	1.1	g/100 g
Serine	0.6	g/100 g
Threonine	0.6	g/100 g
Valine	0.5	g/100 g
VITAMINS		
B2 (Riboflavine)	88	mg/kg
PP (Nicotinic Ac. and nicotinamide)	69	mg/kg
B6 (Pyridoxine)	6	mg/kg
B12 (Cyanocobalamin)	23	μg/kg
Pantotenic Ac.	32	mg/kg
Folate	205	μg/100 g
MINERALS		
Ca	512	mg/100 g
P	5.5	g/100 g
Mg	186	mg/100 g
K	240	mg/100 g
Na	6.1	g/100 g
Zn	2.6	mg/100 g

Proteome profiler mouse cytokine Array Kits were purchased from R&D System (Milan, Italy). $A\beta_{1–42}$ and $A\beta_{42–1}$ peptides were purchased from Tocris (Milan, Italy). For western blot analysis, the primary mouse monoclonal antibodies were obtained from Novus Biologicals (Milan, Italy). Mouse monoclonal anti-actin was obtained from Sigma-Aldrich Co (Milan, Italy). Secondary antibodies (anti-mouse) were purchased from Dako (Copenhagen, Denmark). The mouse transferrin ELISA kit was purchased from Abcam (Cambridge, UK). Unless otherwise stated, all the other reagents were from Carlo Erba (Milan, Italy).

2.2. Animals

CD-1 male mice (10–14 weeks of age, 25–30 g of weight) were purchased from Charles River (Milan, Italy) and kept in an animal care facility under controlled temperature, humidity, and light/dark cycle with food and water *ad libitum*. All animal procedures were performed according to the Declaration of Helsinki (European Union guidelines on the use of animals in scientific experiments), and following ARRIVE guidelines [24,25]. Experimental study groups were randomized and blinded. All procedures were carried out to minimize the number of animals used (N = 7 per group) and their suffering.

2.3. In vivo animal model and drug administration

Mice were randomly separated into 7 experimental groups, as reported in Fig. 1B, balancing body weight variation across groups. For the *in vivo* non-genetic model, we used a well-established AD [26] method consisting of a direct intracerebroventricular (i.c.v.) injection of $A\beta_{1–42}$ fragment. Briefly, before the injection, $A\beta_{1–42}$ protein was dissolved in PBS (1 μg/μl) in tubes that were sealed and incubated for 1 day at 37 °C to allow peptide assembly state. Anesthetized mice (mixture of N_2O and O_2 70:30 w/v containing 2% isoflurane) were then injected with aggregated $A\beta_{1–42}$ peptide (3 μg/3 μl) or its inactive control peptide $A\beta_{42–1}$ (3 μg/3 μl) into cerebral ventricle at a rate of 1 μl/min, using a microsyringe (10 μl, Hamilton) according to the procedure previously [26]. The needle was removed after 3 min using three intermediate steps with 1 min interested delay to minimize backflow. Control group received the surgery procedure and Aβ peptide vehicle injection. After

A

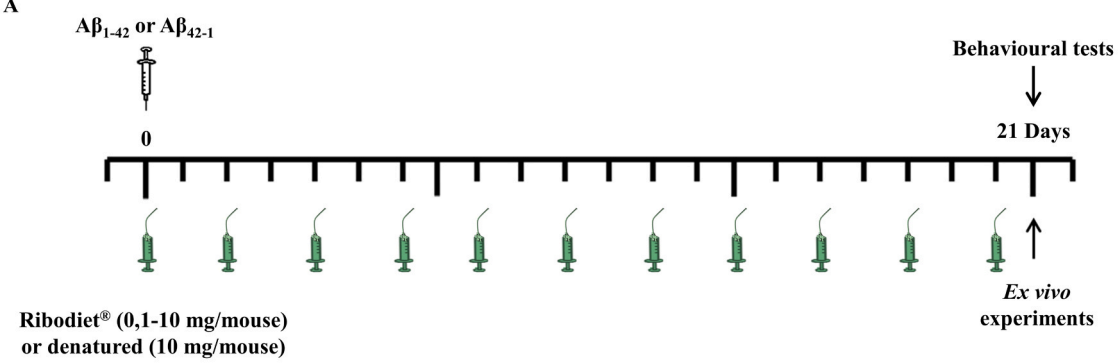

B

Exp. group	Group name	$A\beta_{42-1}$	$A\beta_{1-42}$	Denatured Ribodiet®	Ribodiet®
I	Control	-	-	-	-
II	$A\beta_{42-1}$	3 μg in 3 μl	-	-	-
III	$A\beta_{1-42}$	-	3 μg in 3 μl	-	-
IV	$A\beta_{1-42}$ + Denatured Ribodiet®	-	3 μg in 3 μl	10 mg/mouse	-
V	$A\beta_{1-42}$ + Ribodiet®	-	3 μg in 3 μl	-	0.1 mg/mouse
VI	$A\beta_{1-42}$ + Ribodiet®	-	3 μg in 3 μl	-	1 mg/mouse
VII	$A\beta_{1-42}$ + Ribodiet®	-	3 μg in 3 μl	-	10 mg/mouse

Fig. 1. Schematic representation of experimental plan (behavioral studies and biochemical/molecular analysis) (A) and *in vivo* experimental groups and drug administration (B).

surgery and Aβ administration, mice were placed on a thermal pad until they recovered from the anesthetic. All procedures were performed under strictly aseptic conditions. The Hamilton syringe used for i.c.v. injections was frequently washed with distilled water followed by flushing with 1 mg/ml BSA solution to avoid non-specific binding of peptides to glass. To evaluate the protection profile of the Ribodiet® against $A\beta_{1-42}$ peptide-induced neuro-inflammation, we used oral (p.o.) administration of Ribodiet® (0.1–10 mg/mouse) and its related control (denatured Ribodiet®; 10 mg/mouse) for 21 days (experimental endpoint; Fig. 1A).

2.4. Behavioural studies

21-day-post $A\beta_{1-42}$ administration, mice were tested for novel object recognition (NOR), olfactory discrimination (OD), and Y-maze (Fig. 1A). All tests were performed between 9 a.m. and 2 p.m. in an experimental room with sound isolation. The animals were carried to the test room for, at least, 1 h for acclimation. Behavior was monitored using a video camera positioned above the apparatus, and the videos analysed in a blinded fashion (two operators) using video tracking software (Any-maze, Stoelting, Wood Dale, IL, USA).

2.4.1. Novel object recognition (NOR)

The NOR task exploits a mouse's natural tendency to explore a novel object after previous exposure to two identical objects. Mice were habituated for 10 min into the arena to reduce anxiety associated with the novel arena (plastic arena 30 × 30 × 50 cm). After this habituation stage, mice were ready to perform the task, which was conducted using a familiarization trial (T1) and a test trial (T2) separated by 30 min. During T1, mice could explore for 10 min two identical objects (plastic screw-top tubes) secured to the floor using a small amount of Blu Tack in habituated arenas. For T2, one identical object from T1 was replaced with a novel object (small green flask), and mice could freely explore for 5 min. T1 and T2 were recorded using a video camera and analysed for the time spent interacting with the novel object. All areas were cleaned with 80% ethanol before the test. Novel object exploration was calculated in T2 by (T novel × 100)/(T novel + T identical) with exploration defined as the nose being less than 1 cm from the object when facing the object or actively engaging with the object by sniffing or paw touching. Climbing on the object was not considered exploratory.

2.4.2. Y-maze task

Spontaneous alternation is a measure of spatial working memory. Such short-term working memory was assessed by recording spontaneous alternation behavior during a single session in the Y-maze (made with three arms, 40 cm long, 120° separate) positioned at the exact location for all procedures. Each mouse was placed at the end of one arm and allowed to move freely through the maze during a 5 min session. The series of arm entries were visually recorded. An arm choice was considered only when both forepaws and hind paws fully entered the arm. The Y-maze was cleaned after each test with 80% ethanol to minimize odor cues. Alternation was defined as a successive entrance onto the three different arms. The number of correct entrance sequences (*e.g.*, ABC and BCA) was defined as the number of actual alternations. The number of total possible alternations was, therefore, the total number of arm entries minus two, and the percentage of alternations was calculated as actual alternations / total alternations × 100 [27].

2.4.3. Olfactory discrimination

The task is based on the fact that mice prefer places with their own odor (familiar compartments) instead of places with unfamiliar odors. In this test, mice had access to two adjacent identical chambers separated by an intermediate zone. One chamber contained familiar bedding from its home cage over the last 48 h (familiar), whereas the other contained fresh bedding (non-familiar). Mice were placed individually into the intermediate zone and allowed to explore each chamber for 10 min freely. Rodents can discriminate familiar *versus* non-familiar chambers because they prefer their odor to no odor at all [27]. The time spent in each chamber was recorded and analysed. An olfactory discrimination index was generated according to the following formula: T familiar / (T familiar + T non-familiar), where T equal time and/or 0.5 as final value were considered as no preference.

2.5. Cytokine and chemokine protein array

All mice were sacrificed at the experimental endpoint, and brains were immediately taken. Whole brains were collected into a 2.0 ml tube for immediate preservation in liquid nitrogen and successive storage at − 80 °C. The isolated tissues were homogenized in ice-chilled Tris-HCl buffer (20 mM, pH 7.4) containing 0.32 M sucrose, 1 mM EDTA, 1 mM EGTA, 1 mM PMSF, 1 mM sodium orthovanadate, and one protease inhibitor tablet per 50 ml of buffer. Protein concentration was determined by the BioRad protein assay kit (Bio-Rad, Italy). According to the manufacturer's instructions, equal volumes (1.5 ml) of the pulled homogenates were then incubated with the pre-coated proteome profiler array membranes. Dot plots were detected by using the enhanced chemiluminescence detection kit and Image Quant 400 GE Healthcare software (GE Healthcare, Italy) and successively quantified using GS 800 imaging densitometer software (Biorad, Italy) as previously described [5].

2.6. Western blot analysis

Whole-brain tissue homogenates (35 μg of protein) were subjected to SDS-PAGE (10% gel) using standard protocols, as previously described [28,29]. The proteins were transferred to PVDF membranes in the transfer buffer (25–mM Tris-HCl [pH 7.4] containing 192–mM glycine and 20% v/v methanol) at 400 mA for 2 h. The membranes were saturated by incubation for 2 h with nonfat dry milk (5% wt/v) in PBS supplemented with 0.1% (v/v) Tween 20 (PBS-T) for 2 h at room temperature and then incubated with 1:1000 dilution of anti-$A\beta_{1–42}$, anti-GFAP (glial fibrillary acidic protein), anti-IRP-1 (iron regulatory protein-1), anti-ferritin, anti-TfR-1 or with 1:2000 dilution of anti-Actin (after stripping) overnight at 4 °C and then washed 3 times with PBS-T. Blots were incubated with a 1:3000 dilution of HRP-conjugated secondary Ab for 2 h at room temperature and then washed 3 times with PBS-T. Protein bands were detected using the enhanced chemiluminescence detection kit and Image Quant 400 GE Healthcare software (GE Healthcare, Italy). Protein bands were quantified using GS 800 imaging densitometer software (Biorad, Italy) and normalized with respective actin.

2.7. ELISA assay

Enzyme-linked immunosorbent assays (ELISA) for calcium-binding protein β (S100β) and transferrin were carried out respectively on whole-brain tissue homogenates and serum samples (collected by an intracardiac puncture at experimental endpoint). Briefly, 100 μl of tissue supernatants and 100 μl of serum samples, diluted standards, quality controls, and dilution buffer (blank) were applied on a pre-coated plate with monoclonal anti-S100β and anti-transferrin for 2 h. After washing, 100 μl of biotin labeled antibody was added for each plate, and incubation continued for 1 h. The plates were washed, and 100 μl of streptavidin-HRP conjugate was added, and the plates were incubated for a further 30 min period in the dark. The addition of 100 μl of the substrate and stop solution represented the last steps before the absorbance reading (measured at 450 nm) on a microplate reader. S100β and transferrin levels in the samples were determined respectively using a standard curve of S100β [26], expressed as μg/ml, and a standard curve of transferrin [5], expressed as mg/dl.

2.8. Haematological investigations

Standard laboratory procedures were used for blood sampling and measurements [30]. Haematological investigations, for all experimental conditions, including blood count test, leukocyte, and sidereal formula were performed on citrated and not-anticoagulated blood samples, respectively. Serological tests were performed by CELL-DYN Sapphire purchased from Abbott S.r.l. (Milan, Italy). All procedures were conducted under strictly aseptic conditions.

2.9. Data and statistical analysis

The data and statistical analysis in this study comply with the international recommendations on experimental design and analysis in pharmacology [31] and data sharing and presentation in preclinical pharmacology [32,33]. The results obtained were expressed as the mean ± SEM. Statistical analysis was performed by using one-way, or two-way ANOVA followed by Dunnett's or Bonferroni's for multiple comparisons. GraphPad Prism 8.0 software (San Diego, CA, USA) was used for analysis. Differences between means were considered statistically significant when $P \leq 0.05$ was achieved. Sample size was chosen to ensure alpha 0.05 and power 0.8. Animal weight was used for randomization and group allocation to reduce unwanted sources of variations by data normalization. No animals and related *ex vivo* samples were excluded from the analysis. *In vivo* and *in vitro* studies were carried out to generate groups of equal size (N = 7 of independent values), using randomization and blinded analysis.

3. Results

3.1. Ribodiet® alleviates the $A\beta_{1–42}$-induced memory decline and learning deficit

Consistent with the demonstration that olfactory dysfunction occurs at the early stage of Aβ-induced pathology, the administration of $A\beta_{1–42}$ (3 μg/3 μl, i.c.v.) significantly decreased the capability of mice to discriminate new and familiar odors, when examined in the olfactory discrimination test compared to Control ($P \leq 0.01$ *vs* Ctrl, Fig. 2A) and $A\beta_{42–1}$ groups (data not shown). Interestingly, administration of Ribodiet® (0.1–10 mg/mouse, p.o.) was shown to significantly attenuate the olfactory dysfunction at 21 days following $A\beta_{1–42}$ administration ($P \leq 0.05$ *vs* $A\beta_{1–42}$, Fig. 2A). Consistently, administration of $A\beta_{1–42}$ reduced the delta time in the novel Object Recognition (NOR) test ($P \leq 0.01$ *vs* Ctrl, Fig. 2B), whereas Ribodiet® significantly attenuated the $A\beta_{1–42}$-related impairment (Fig. 2B). Furthermore, the possible neuroprotective effects of Ribodiet® was evaluated on the $A\beta_{1–42}$-induced learning deficits. The percentage of correct alternations in the Y-maze test was then analysed on day 21 after $A\beta_{1–42}$ injection. $A\beta_{1–42}$ fragment induced a significant impairment of spontaneous alternation performances in Y-maze test compared to Control ($P \leq 0.05$ *vs* Ctrl, Fig. 2C) and $A\beta_{42–1}$ group (data not shown). Remarkably, Ribodiet® administrated at the higher doses of 1.0 and 10 mg/mouse (p.o.) resulted in a significant ($P \leq 0.05$) attenuation of the $A\beta_{1–42}$-induced spontaneous alternation impairments (Fig. 2C). No significant differences were found in the total number of arm entries (Fig. 2D).

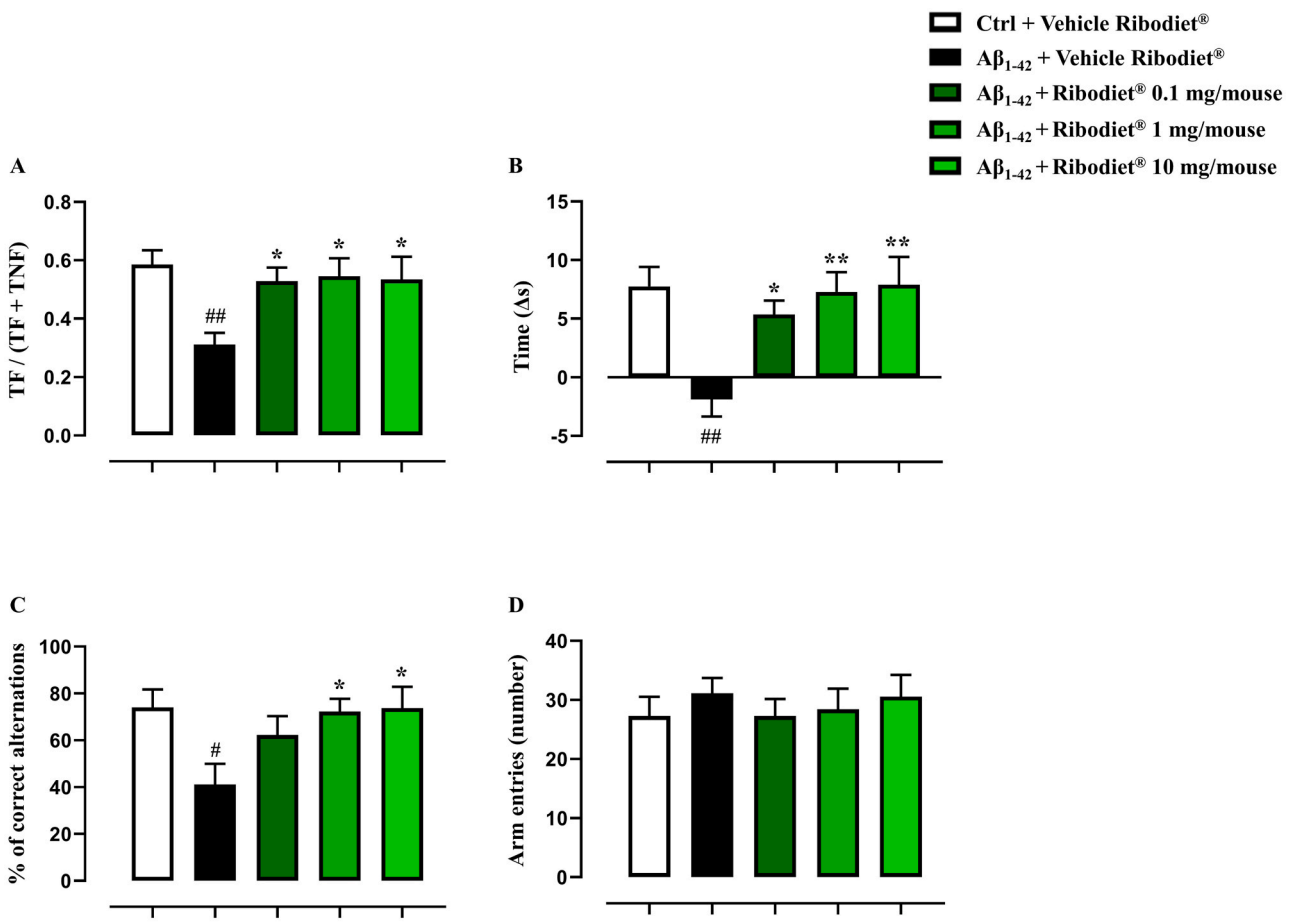

Fig. 2. Neuroprotective effect of Ribodiet® at the doses of 0.1, 1 and 10 mg/mouse on olfactory discrimination test (A), object recognition test (B), $A\beta_{1-42}$-induced spontaneous alternation deficits in mice (C), and for total number of arm entries in Y-maze test (D). Mice were injected intracerebroventricularly (i.c.v.) with PBS (3 μl; Ctrl), i.c.v. $A\beta_{1-42}$ peptide (3 μg/3 μl), or i.c.v. $A\beta_{1-42}$ peptide (3 μg/3 μl) + Ribodiet® (0.1–10 mg/mouse). After 21 days, mice were examined for the time spent in familiar (TF) or unfamiliar (TNF) chamber (A), Delta (Δ) of time with a familiar or a novel object (B), spontaneous alternation in the Y-maze apparatus (C-D). The results obtained were expressed as the mean ± SEM. Statistical analysis was conducted by using one-way ANOVA followed by Bonferroni's for multiple comparisons. $^{\#}P \leq 0.05$, $^{\#\#}P \leq 0.01$ *vs* Ctrl-treated group; $^{*}P \leq 0.05$, $^{**}P \leq 0.01$ *vs* $A\beta_{1-42}$ peptide-treated group (N = 7 per group).

3.2. Ribodiet® reduces mice reactive gliosis by the reduction of GFAP and S100β

We began our biochemical analysis by confirming the behavioral findings associated with $A\beta_{1-42}$ levels by western blot analysis on whole-brain tissue homogenates (Fig. 3A). As expected, $A\beta_{1-42}$ levels were significantly higher in the $A\beta_{1-42}$ group compared to Control ($P \leq 0.005$ *vs* Ctrl, Fig. 3A and C), while no significant modulation was observed after Ribodiet® treatment. Based on these findings, we decided to examine the expression of GFAP and S100β as markers of reactive gliosis to evaluate the potential neuroprotective effects of Ribodiet®. Interestingly, we found that the administration of $A\beta_{1-42}$ induced a significant increase of GFAP protein compared to Control-treated mice ($P \leq 0.01$ *vs* Ctrl Fig. 3A and B). Remarkably, the levels of GFAP were significantly attenuated after Ribodiet® treatment at the dose of 1 and 10 mg/mouse ($P \leq 0.01$ *vs* $A\beta_{1-42}$, Fig. 3B). Uncropped and original western blots are presented in Supplementary Fig. 4**.** According to these results, we observed that the administration of $A\beta_{1-42}$ provoked a marked and significant increase of S100β expression compared to Control group ($P \leq 0.01$ *vs* Ctrl Fig. 3D), while treatment with Ribodiet® (1–10 mg/mouse, p.o.) decreased the increase of this protein in mice brain homogenates ($P \leq 0.05$ *vs* $A\beta_{1-42}$, Fig. 3D).

3.3. Ribodiet® decreases mice neuro-inflammation by modulation of pro-inflammatory cyto-chemokines

We next analysed the cytokine and chemokine profile from total brain homogenates of selected experimental groups. In line with our *in vivo* evidence, Fig. 4 shows that the administration of Ribodiet® induced a selective reversal of pro-inflammatory onset (Fig. 4A–D). Densitometric analysis revealed that Ribodiet® at the higher doses of 1 and 10 mg/mouse (p.o.) induced a specific modulation (Fig. 4E) in the following factors: CXCL-13 ($P \leq 0.001$), CXCL-1 ($P \leq 0.001$), IL-1α ($P \leq 0.001$), IL-1Ra ($P \leq 0.001$), IL-16 ($P \leq 0.001$), keratinocyte-derived cytokine (KC; $P \leq 0.001$), macrophage inflammatory protein (MIP)-1α ($P \leq 0.001$), MIP-2 ($P \leq 0.001$), tissue inhibitors of metalloproteinase (TIMP)-1 ($P \leq 0.001$), triggering receptor expressed on myeloid cells-1 (TREM-1; $P \leq 0.001$), complement component 5a (C5a; $P \leq 0.05$ for Ribodiet® 10 mg/mouse), ICAM-1 ($P \leq 0.05$; $P \leq 0.001$ respectively for Ribodiet® 1 and 10 mg/mouse) and stromal derived factor-1 (SDF-1; $P \leq 0.001$) compared to $A\beta_{1-42}$ group. A similar inhibitory profile was found for Ribodiet® at the lowest dose of 0.1 mg/mouse for the following cyto-chemokines: CXCL-1 ($P \leq 0.001$), IL-1Ra ($P \leq 0.001$), KC ($P \leq 0.001$), MIP-1α ($P \leq 0.001$), MIP-2 ($P \leq 0.001$), TIMP-1 ($P \leq 0.05$), TREM-1 ($P \leq 0.001$) and SDF-1 ($P \leq 0.01$) (Fig. 4E).

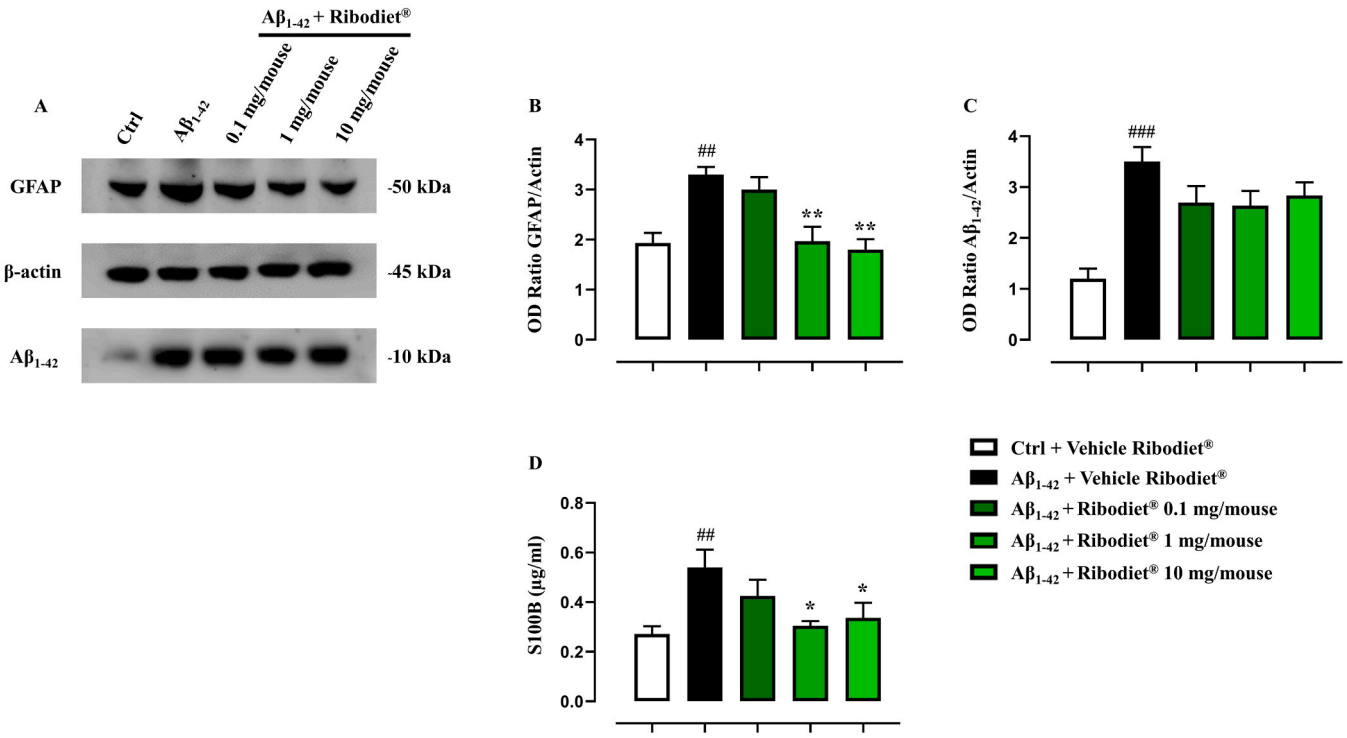

Fig. 3. Representative western blotting (A) and related cumulative densitometric analyses of GFAP (B) and $A\beta_{1–42}$ (C) proteins in whole brain tissue homogenates from mice injected intracerebroventricularly (i.c.v.) with PBS (3 μl; Ctrl), i.c.v. $A\beta_{1–42}$ peptide (3 μg/3 μl), or i.c.v. $A\beta_{1–42}$ peptide (3 μg/3 μl) + Ribodiet® (0.1–10 mg/mouse). Values are presented as means ± SEM of three separate independent experiments run each with N = 7 mice per group pooled. Statistical analysis was conducted by one-way ANOVA followed by Bonferroni's for multiple comparisons. $^{\#\#}P \leq 0.01$, $^{\#\#\#}P \leq 0.005$ *vs* Ctrl-treated group; $^{**}P \leq 0.01$ *vs* $A\beta_{1–42}$ peptide-treated group. Effect of Ribodiet®, in all tested doses, on the release of S100β protein (detected by ELISA assay and expressed as μg/ml) in total brain homogenates (D). The results obtained were expressed as the mean ± SEM. Statistical analysis was performed by using one-way ANOVA followed by Bonferroni's for multiple comparisons. $^{\#\#}P \leq 0.01$ *vs* Ctrl-treated group; $^{*}P \leq 0.05$ *vs* $A\beta_{1–42}$ peptide-treated group (N = 7 per group).

3.4. Effect of Ribodiet® on $A\beta_{1–42}$-induced alteration of haematological parameters

Considering that AD is commonly associated with a perturbation of circulating iron metabolism, we next analysed the effect of Ribodiet® on the biochemical indicators of iron homeostasis and related haematological parameters. As shown in Table 2, the administration of $A\beta_{1–42}$ induced a significant increase of sideremia (expressed as μg/dl) compared to Control ($P \leq 0.01$ *vs* Ctrl, Table 2) and $A\beta_{42–1}$ groups (data not shown). Remarkably, the levels of sideremia were significantly attenuated after the administration of Ribodiet® at the dose of 1 and 10 mg/mouse ($P \leq 0.01$ *vs* $A\beta_{1–42}$); whereas no significant differences were found for serum concentrations of transferrin (mg/dl) in all experimental groups (Table 2). Interestingly, we observed that the administration of $A\beta_{1–42}$ provoked a marked and significant decrease of red blood cells (expressed as 10^6/μl; $P \leq 0.01$ *vs* Ctrl), haemoglobin (expressed as g/dL; $P \leq 0.05$ *vs* Ctrl), and haematocrit (expressed as %; $P \leq 0.01$ *vs* Ctrl) compared to Control and $A\beta_{42–1}$ groups (data not shown), while treatment with Ribodiet® (1–10 mg/mouse) significantly reverted the reduction of these haematological parameters in mice serum samples (red blood cells: $P \leq 0.01$; haemoglobin: $P \leq 0.05$; haematocrit: $P \leq 0.01$ *vs* $A\beta_{1–42}$; Table 2). Moreover, our results showed that the administration of $A\beta_{1–42}$ did not induce significant variances of haematologic indices of white blood cells (expressed as 10^3/μl) and platelets (expressed as 10^3/μl) (Table 2), as well as total leucocyte formula (neutrophils, monocytes, lymphocytes, eosinophils, basophils) (Supplementary Table 1).

3.5. Effect of Ribodiet® on $A\beta_{1–42}$-induced alteration of brain iron homeostasis

Based on previous results, we decided to examine the expression of proteins involved in iron regulation (IRP-1), its uptake (TfR-1), and storage (ferritin). As reported in Fig. 5, western blot analysis performed on total brain homogenates shown a significant increase of TfR-1 expression in $A\beta_{1–42}$-treated group ($P \leq 0.01$ *vs* Ctrl, Fig. 5A and C) and a significant reduction after Ribodiet® treatment at the higher doses of 1 ($P \leq 0.05$) and 10 mg/mouse ($P \leq 0.01$) (Fig. 5A and C).

The results observed in terms of TfR-1 expression were also confirmed by a specular and significant modulation of ferritin levels ($P \leq 0.01$ *vs* Ctrl; $P \leq 0.05$ and $P \leq 0.01$ *vs* $A\beta_{1–42}$, respectively for Ribodiet® 1 mg/mouse and Ribodiet® 10 mg/mouse, Fig. 5A and D). However, no significant effects were observed in $A\beta_{1–42}$ and Ribodiet®-treated groups in term of IRP-1 expression (Fig. 5A and B). Uncropped and original western blots are presented in Supplementary Fig. 5.

4. Discussion

Alzheimer is the most common and one of the most studied neurodegenerative disorder [1]. It has become a critical issue to human health, especially in aging societies, and therefore, it is a focus of research in the global scientific community [34]. It is a multifactorial disorder primarily characterized by the deposition of amyloid plaques in the brain, leading to irreversible cognitive impairment and neuro-inflammation that mainly involves hippocampus and cortex districts [35].

Different research studies in the field of age-cognitive diseases have been conducted to discover how the brain degenerates and the importance of "nutritional determinant" in AD onset and development [36]. In

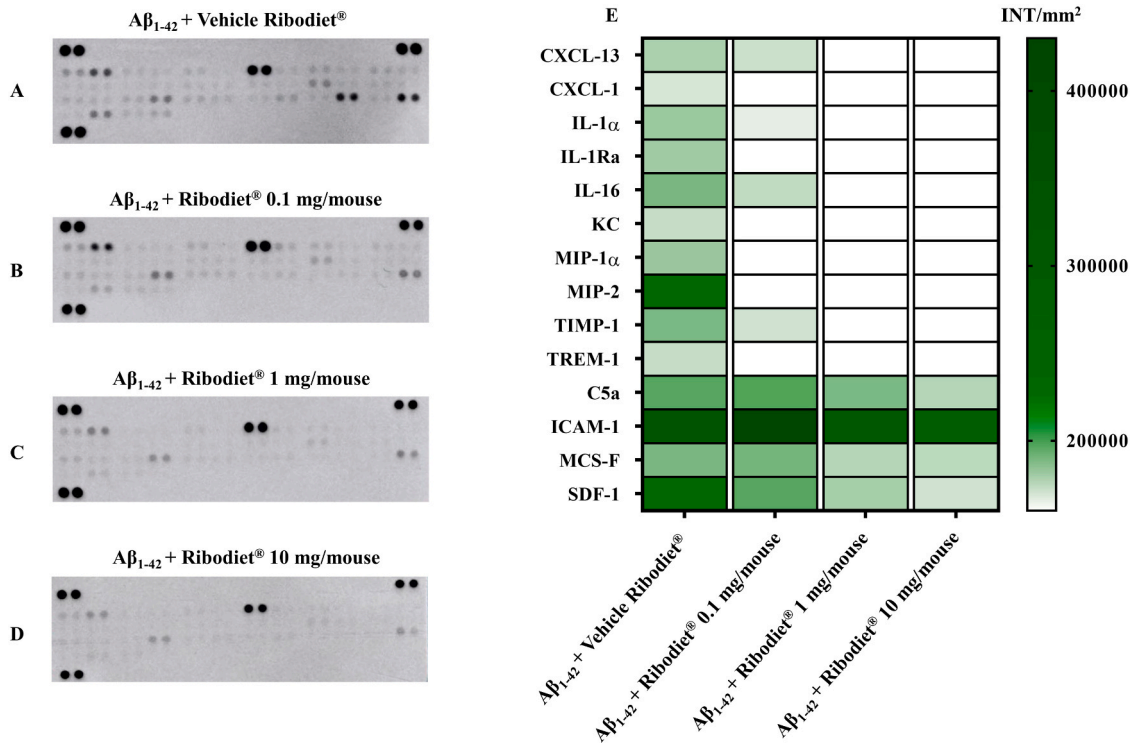

Fig. 4. Inflammatory fluids obtained from total brain homogenates, after 21 days of treatment of $A\beta_{1-42}$ + Vehicle Ribodiet® (A), $A\beta_{1-42}$ + Ribodiet® 0.1 mg/mouse (B), $A\beta_{1-42}$ + Ribodiet® 1 mg/mouse (C), $A\beta_{1-42}$ + Ribodiet® 10 mg/mouse-treated mice (D) were assessed using a proteome profiler cytokine array panel and presented as heatmap for their related densitometric analysis (E). Data (expressed as INT/mm^2) are presented as the mean ± SEM of positive spots of three independent experiments run each with N = 7 mice per group pooled. Statistical analysis (reported in the text) was performed by using two-way ANOVA followed by Dunnett's for multiple comparisons. *P ≤ 0.05, **P ≤ 0.01, ****P ≤ 0.001 *vs* $A\beta_{1-42}$ peptide-treated group (N = 7 per group).

Table 2
Serum samples collected by intracardiac puncture of Ctrl + Vehicle Ribodiet®, $A\beta_{1-42}$ + Vehicle Ribodiet®, $A\beta_{1-42}$ + Ribodiet® (0.1–10 mg/mouse)-treated mice were assessed for haematological parameters (white blood cells, red blood cells, haemoglobin, haematocrit, and platelets) and biochemical indicators of iron homeostasis (sideremia, transferrin). Results obtained were expressed as the mean ± SEM. Statistical analysis was performed by using one-way ANOVA followed by Bonferroni's for multiple comparisons. $^{\#}P \leq 0.05$, $^{\#\#}P \leq 0.01$ *vs* Ctrl-treated group; *P ≤ 0.05, **P ≤ 0.01 *vs* $A\beta_{1-42}$ peptide-treated group (N = 7 mice per group).

Parameters	Control	$A\beta_{1-42}$	$A\beta_{1-42}$ + Ribodiet® 0.1 mg/mouse	$A\beta_{1-42}$ + Ribodiet® 1 mg/mouse	$A\beta_{1-42}$ + Ribodiet® 10 mg/mouse
Sideremia (μg/dL)	273.70 ± 56.08	973.10 ± 87.57$^{\#\#}$	1103.00 ± 215.10	357.00 ± 88.38**	327.90 ± 78.96**
Transferrin (mg/dL)	48.71 ± 5.85	41.00 ± 1.00	48.14 ± 5.31	43.63 ± 3.62	47.31 ± 4.75
White blood cells (10^3/μl)	10.87 ± 0.98	13.37 ± 1.19	12.12 ± 1.43	14.44 ± 2.01	13.22 ± 2.02
Red blood cells (10^6/μl)	14.08 ± 0.65	9.74 ± 0.68$^{\#\#}$	7.34 ± 1.24	14.16 ± 0.76**	14.36 ± 1.07**
Hemoglobin (g/dL)	24.19 ± 0.89	19.60 ± 0.96$^{\#}$	17.50 ± 1.49	23.84 ± 0.71*	24.20 ± 0.67*
Hematocrit (%)	77.67 ± 3.41	48.76 ± 4.85$^{\#\#}$	39.40 ± 8.50	77.93 ± 2.10**	75.89 ± 4.20**
Platelets (10^3/μl)	894.10 ± 149.30	1249.00 ± 201.40	988.00 ± 88.18	818.40 ± 124.70	997.30 ± 90.53

this context, comprehensive literature research reveals evidence linking the consumption of essential nutrients to preventing the disease conditions that result in cognitive decline and how a "nutraceutical approach" could stimulate neuroprotection mechanisms and regulate risk factors in neurodegenerative diseases [37,38].

Based on these evidences, here we examined the potential protective effect of Ribodiet® in the onset of $A\beta_{1-42}$-induced neuro-inflammation. The main finding in this study is that Ribodiet® can reverse *in vivo* the memory deficits of AD, and suppress the reactive gliosis and neuroinflammation. In detail, for the first time, our results show that Ribodiet® rescues the memory performance decline in $A\beta_{1-42}$-induced AD in the main behavioural and mnemonic tests (Y-maze, Object Recognition, Olfactory discrimination), without interfering with their motor activity.

Besides, Ribodiet® reverses reactive gliosis and neuro-inflammation, as indicated *ex vivo* by the reduced production of S100β, a glial-derived protein that is mainly secreted from activated astrocytes and microglia [39–41]. S100β, at low concentrations, is considered a neurotrophic factor and neuronal survival protein during the development of the nervous system [42]. Conversely, when overproduced by activated glia, this protein becomes a mediator of pathology, influencing disease progression by acting as a pro-inflammatory cytokine, thus contributing to the exacerbation of neuro-inflammation and neuronal dysfunction [43]. In addition, S100β production can be stimulated by mediators associated with AD, including β-amyloid and pro-inflammatory cytokines [42]. Collectively, this highlights the crucial role of S100β in AD onset and progression, and the relevant effects of Ribodiet® in reducing its expression in mouse whole brain. Contextually, it is essential to underline that, in this scenario, astrocytes (a subtype of glial cells) can change into a so-called reactive state of astrogliosis characterized by the increased expression of GFAP that lead to the formation of amyloid plaques and, to a lesser extent, neurofibrillary tangles [40,44]. The western blot analysis of GFAP performed on brain tissue indicates that

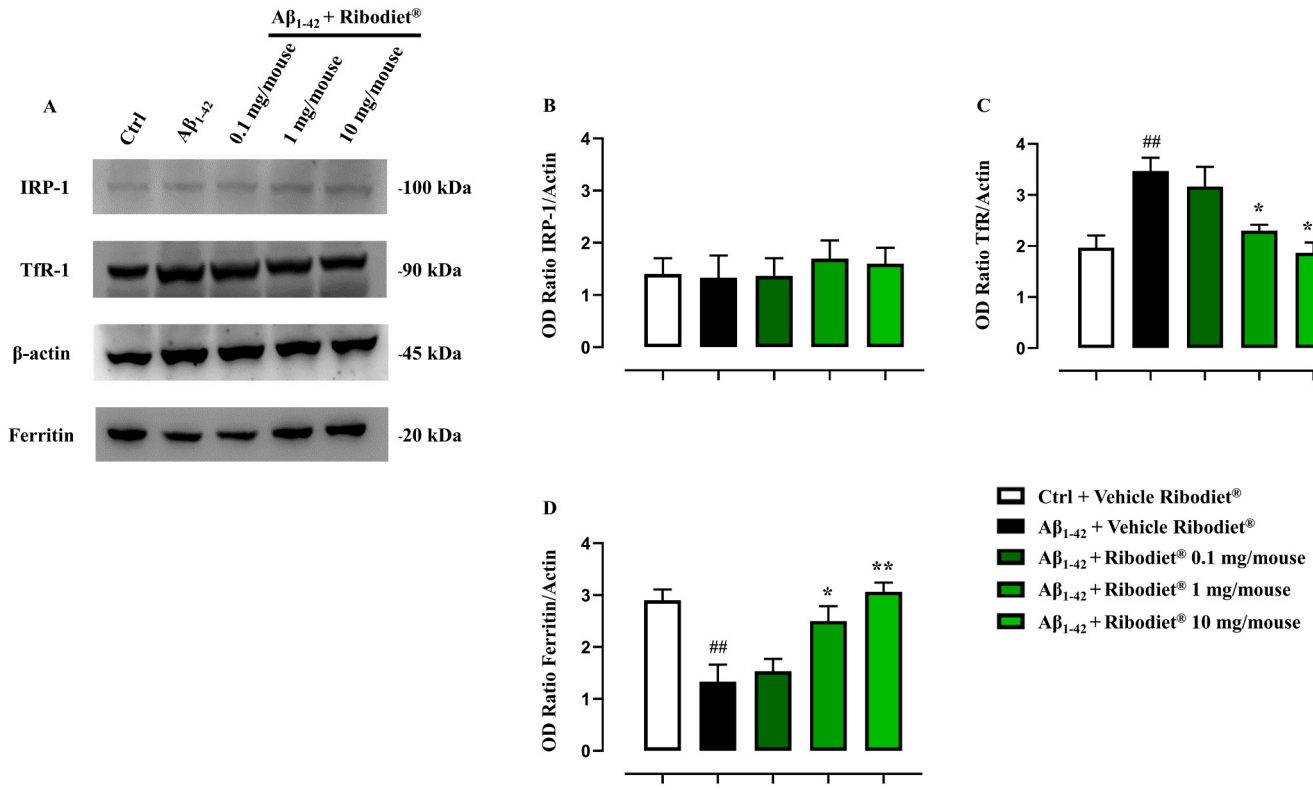

Fig. 5. Representative western blotting (A) and related cumulative densitometric analyses of IRP-1 (B), TfR-1 (C), ferritin proteins (D) in whole brain tissue homogenates from mice injected intracerebroventricularly (i.c.v.) with PBS (3 μl; Ctrl), i.c.v. $A\beta_{1-42}$ peptide (3 μg/3 μl), or i.c.v. $A\beta_{1-42}$ peptide (3 μg/3 μl) + Ribodiet® (0.1–10 mg/mouse). Values are presented as means ± SEM of three separate independent experiments run each with N = 7 mice per group pooled. Statistical analysis was conducted by using one-way ANOVA followed by Bonferroni's for multiple comparisons. $^{\#\#}P \leq 0.01$ *vs* Ctrl-treated group; $^{*}P \leq 0.05$, $^{**}P \leq 0.01$ *vs* $A\beta_{1-42}$ peptide-treated group.

Ribodiet®-treated animals shown a significant reduction of this fibrillary protein that may lastly reduce the number of neurofibrillary tangles in mice AD brain.

In line with our previous studies [5,26], to strengthen and better analyse the neuro-protective effects of Ribodiet®, we also monitored the level of typical pro-inflammatory cyto-chemokines that are normally up-regulated during pathology onset and progression [45–48]. Accordingly, we found an elevated expression of different pro-inflammatory mediators such as IL-1α, IL-1Ra, IL-16, CXCL-1, CXCL-13, MIP-1α, TIMP-1, TREM-1, ICAM-1, SDF-1, MIP-2 cytokines, and chemokines in the brain of Aβ-treated mice. Interestingly, we report, for the first time, a significant reduction of these pro-inflammatory cascades after Ribodiet® treatment suggesting a modulation of the key cyto-chemokines released from activated astrocytes and microglia involved in neuron protections and cognitive behaviors [5].

Another important physio-pathological aspect of AD is the oxidative damage and cell death [49,50] that in many neurological diseases, including Parkinson's disease, Alzheimer's disease, amyotrophic lateral sclerosis, and others seem to be related to iron accumulation [51,52]. Iron is essential for the brain's normal development and functions; however, excess redox-active iron can lead to oxidative damage and neuronal death. Indeed, cellular iron level on central nervous system (CNS) is tightly regulated and modulated [53,54]. For these reasons, new strategies of therapy indicate that Fe^{2+} chelator may be a new target for AD disorders [55]. For instance, Tf constitutes a family of Fe-binding proteins that transport iron into the endosomal compartment of cells by forming complexes of Fe-bound Tf and the TfR [56]. Once Fe^{2+} is released from transferrin, it is known to induce the generation of oxygen radicals, which in turn stimulate the production of toxic Aβ oligomers [57]. Here, we shown that the levels of this transporter were not altered but, contextually, we observed a specular modulation of the TfR-1 and ferritin proteins (proteins implicated in iron uptake and storage respectively), thus highlighting the neuroprotective effect of Ribodiet®.

Finally, it has been reported that perturbation of iron homeostasis in the brain is reflected peripherally by specific haematological values [13,14]. Accordingly, Faux and coll. [15] demonstrated that AD patients have significantly lower haemoglobin level compared to healthy patients and a pathological change of transferrin-haemoglobin ratio, as a consequent alteration of iron transportation to bone marrow [15]. Our results confirmed these evidences and, according to haematological analyses, we observed in $A\beta_{1-42}$-treated mice a reduction of the main parameters involved in iron peripheral homeostasis such as red blood cells, haematocrit, and haemoglobin. This circulant imbalance, correlated to the development of reactive oxygen species and neuro-inflammation, was completely reversed by the administration of high doses of Ribodiet®.

5. Conclusion

In conclusion, the experimental findings reported here confirm and extend previous data showing that oxidative stress, neuro-inflammation, and iron dysregulation are the detrimental factor for AD, where this element could represent a key factor for the "self-amplifying" neuro-inflammatory onset typical of Aβ-related disease (Fig. 6). Moreover, for the first time, we present a complete "picture" of how a supplementation with ribonucleotide-based ingredient (Ribodiet®) can lessen oxidative stress, brain inflammation and, amyloid pathology in a non-genetic mouse model of Alzheimer. However, future studies and clinical evidence will need to extend the protective role exerted by Ribodiet®, as a natural modulator of the developmental neuro-toxicity of AD.

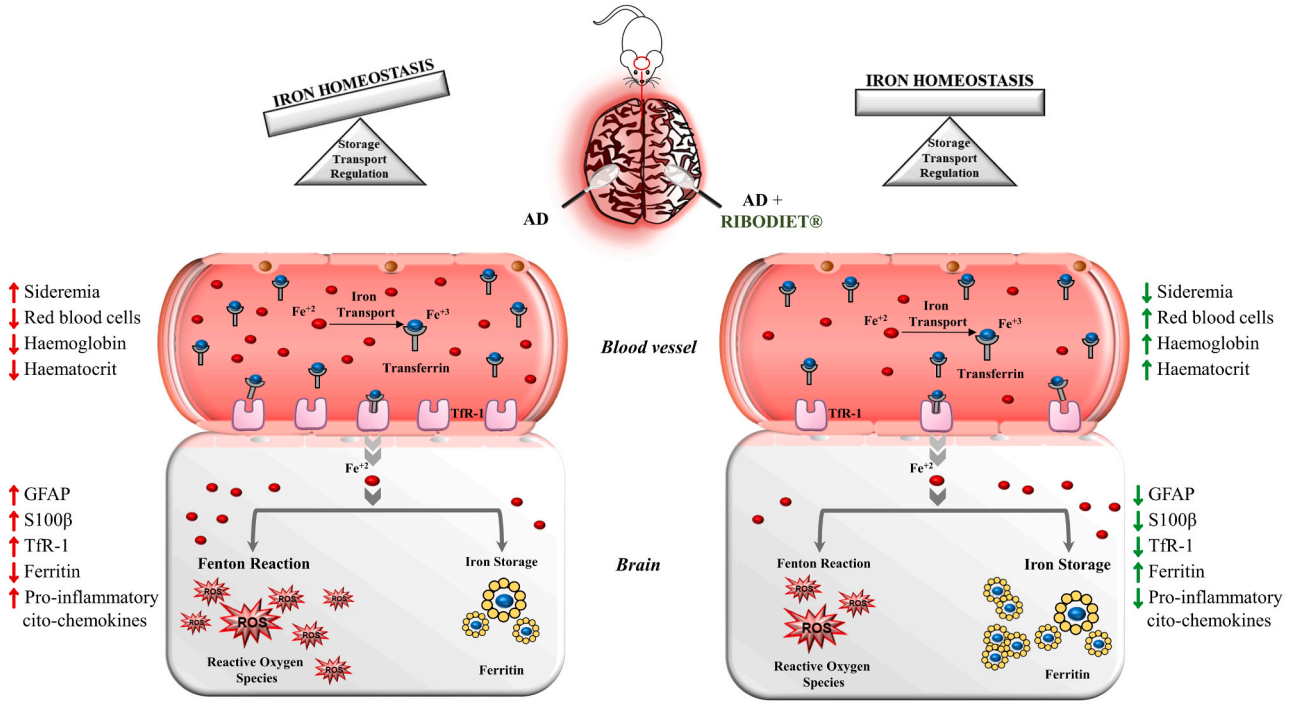

Fig. 6. Schematic representation of the effects of a ribonucleotide-based ingredient Ribodiet® in a non-genetic mouse model of AD. Ribodiet® alleviates memory decline, neuro-inflammation, and oxidative stress *via* modulation of iron-related metabolic proteins paving the way for its rationale use for the treatment and/or prevention of AD and other age-related diseases.

Patents

Industrial invention patent "Composition comprising 5'-ribonucleotides for use in the treatment of Alzheimer's disease". N: 102019000013044. Inventors: Maione Francesco, Daglia Maria, Raucci Federica, Saviano Anella, Bonvicini Daniele and Sgherbini Alessandro.

Author contributions

A.S., G.M.C., F.R., A.P., C.S., M.P. and M.G.F. performed the experiments. M.D., N.M. and F.M. drafted and wrote the manuscript. M.C., A. S., N.P., D.B, N.M analysed data and revised the manuscript. All Authors gave final approval to the publication.

Conflict of interest statement

This article has been conducted and written in the absence of any commercial or financial relationships that could be construed as a potential conflict of interest.

Acknowledgments

This work was supported by PROSOL S.p.A, Italy. (Convenzione "Identificazione e dimostrazione di efficacia tera-peutica di Ribodiet® per il controllo delle forme di demenza senile" Protocol Number: 2018/0058554).

Appendix A. Supporting information

Supplementary data associated with this article can be found in the online version at doi:10.1016/j.biopha.2021.111579.

References

[1] Z. Liu, A. Zhang, H. Sun, Y. Han, L. Kong, X. Wang, Two decades of new drug discovery and development for Alzheimer's disease, RSC Adv. 7 (2017) 6046–6058, https://doi.org/10.1039/C6RA2673H.
[2] R. Bronzuoli, A. Iacomino, L. Steardo, C. Scuderi, Targeting neuroinflammation in Alzheimer's disease, J. Inflamm. Res. 9 (2016) 199–208, https://doi.org/10.2147/JIR.S86958.
[3] R.A. Huynh, C. Mohan, Alzheimer's disease: biomarkers in the genome, blood, and cerebrospinal fluid, Front. Neurol. 8 (2017) 102, https://doi.org/10.3389/fneur.2017.00102.
[4] P. Scheltens, K. Blennow, M.M. Breteler, B. de Strooper, G.B. Frisoni, S. Salloway, W.M. Van der Flier, Alzheimer's disease, Lancet 388 (2016) 505–517, https://doi.org/10.1016/s0140-6736(15)01124-1.
[5] C. Cristiano, F. Volpicelli, P. Lippiello, B. Buono, F. Raucci, M. Piccolo, A.J. Iqbal, C. Irace, M.C. Miniaci, C. Perrone Capano, A. Calignano, N. Mascolo, F. Maione, Neutralization of IL-17 rescues amyloid-β-induced neuroinflammation and memory impairment, Br. J. Pharmacol. 176 (18) (2019) 3544–3557, https://doi.org/10.1111/bph.14586.
[6] I. Baldeiras, I. Santana, M.T. Proença, M.H. Garrucho, R. Pascoal, A. Rodrigues, D. Duro, C.R. Oliveira, Peripheral oxidative damage in mild cognitive impairment and mild Alzheimer's disease, J. Alzheimers Dis. 15 (2008) 117–128, https://doi.org/10.3233/jad-2008-15110.
[7] N. Singh, S. Haldar, A.K. Tripathi, K. Horback, J. Wong, D. Sharma, A. Beserra, S. Suda, C. Anbalagan, S. Dev, C.K. Mukhopadhyay, A. Singh, Brain iron homeostasis: from molecular mechanisms to clinical significance and therapeutic opportunities, Antioxid. Redox Signal. 20 (8) (2014) 1324–1363, https://doi.org/10.1089/ars.2012.4931.
[8] L. Zecca, M.B. Youdim, P. Riederer, J.R. Connor, R.R. Crichton, Iron, brain ageing and neurodegenerative disorders, Nat. Rev. Neurosci. 5 (11) (2004) 863–873, https://doi.org/10.1038/nrn1537.
[9] K. Jomova, M. Valko, Advances in metal-induced oxidative stress and human disease, Toxicology 283 (2–3) (2011) 65–87, https://doi.org/10.1016/j.tox.2011.03.001.
[10] Z. Liu, T. Zhou, A.C. Ziegler, P. Dimitrion, L. Zuo, Oxidative stress in neurodegenerative diseases: from molecular mechanisms to clinical applications, Oxid. Med. Cell. Longev. 2017 (2017) 1–11, https://doi.org/10.1155/2017/2525967.
[11] A. Carocci, A. Catalano, M.S. Sinicropi, G. Genchi, Oxidative stress and neurodegeneration: the involvement of iron, Biometals 31 (5) (2018) 715–735, https://doi.org/10.1007/s10534-018-0126-2.
[12] B.B. Muhoberac, R. Vidal, Iron, ferritin, hereditary ferritinopathy, and neurodegeneration, Front. Neurosci. 13 (2019) 1195, https://doi.org/10.3389/fnins.2019.01195.

[13] R.C. Shah, R.S. Wilson, Y. Tang, X. Dong, A. Murray, D.A. Bennett, Relation of hemoglobin to level of cognitive function in older persons, Neuroepidemiology 32 (2009) 40–46, https://doi.org/10.1159/000170905.
[14] J.D. Doecke, S.M. Laws, N.G. Faux, W. Wilson, S.C. Burnham, C.P. Lam, A. Mondal, J. Bedo, A.I. Bush, B. Brown, K. De Ruyck, K.A. Ellis, C. Fowler, V.B. Gupta, R. Head, S.L. Macaulay, K. Pertile, C.C. Rowe, A. Rembach, M. Rodrigues, R. Rumble, C. Szoek, K. Taddei, T. Taddei, B. Trounson, D. Ames, C.L. Masters, R. N. Martins, Alzheimer's Disease Neuroimaging Initiative, Australian Imaging Biomarker and Lifestyle Research Group, Blood-based protein biomarkers for diagnosis of Alzheimer disease, Arch. Neurol. 69 (10) (2012) 1318–1325, https://doi.org/10.1001/archneurol.2012.1282.
[15] N.G. Faux, A. Rembach, J. Wiley, K.A. Ellis, D. Ames, C.J. Fowler, R.N. Martins, K. K. Pertile, R.L. Rumble, B. Trounson, C.L. Masters, A.I. AIBL Research Group; Bush, An anemia of Alzheimer's disease, Mol. Psychiatry 19 (11) (2014) 1227–1234, https://doi.org/10.1038/mp.2013.178.
[16] J.T. Neary, M.P. Rathbone, F. Cattabeni, M.P. Abbracchio, G. Burnstock, Trophic actions of extracellular nucleotides and nucleosides on glial and neuronal cells, Trends Neurosci. 19 (1996) 13–18, https://doi.org/10.1016/0166-2236(96)81861-3.
[17] F.F. Ribeiro, S. Xapelli, C. Miranda-Lourenço, S.R. Tanqueiro, J. Fonseca-Gomes, M.J. Diógenes, J.A. Ribeiro, A.M. Sebastião, Purine nucleosides in neuroregeneration and neuroprotection, Neuropharmacology 104 (2015) 226–242, https://doi.org/10.1016/j.neuropharm.2015.11.006.
[18] P. Alonso-Andrès, J.L. Albasanz, I. Ferrer, M. Martín, Purine-related metabolites and their converting enzymes are altered in frontal, parietal and temporal cortex at early stages of Alzheimer's disease pathology, Brain Pathol. 28 (6) (2018) 933–946, https://doi.org/10.1111/bpa.12592.
[19] N. Braidy, R. Grant, P.S. Sachdev, Nicotinamide adenine dinucleotide and its related precursors for the treatment of Alzheimer's disease, Curr. Opin. Psychiatry 31 (2) (2018) 160–166, https://doi.org/10.1097/YCO.0000000000000394.
[20] M.P. Rathbone, P.J. Middlemiss, J.W. Gysbers, C. Andrew, M.A. Herman, J. K. Reed, R. Ciccarelli, P. Di Iorio, F. Caciagli, Trophic effects of purines in neurons and glial cells, Prog. Neurobiol. 59 (1999) 663–690, https://doi.org/10.1016/S0301-0082(99)00017-9.
[21] R. Ciccarelli, P. Ballerini, G. Sabatino, M.P. Rathbone, M. D'Onofrio, F. Caciagli, P. Di Iorio, Involvement of astrocytes in purine-mediated reparative processes in the brain, Int. J. Dev. Neurosci. 19 (4) (2001) 395–414, https://doi.org/10.1016/s0736-5748(00)00084-8.
[22] L.E. Bettio, J. Gil-Mohapel, A.L. Rodrigues, Guanosine and its role in neuropathologies, Purinergic Signal. 12 (3) (2016) 411–426, https://doi.org/10.1007/s11302-016-9509-4.
[23] ⟨http://www.ema.europa.eu/docs/en_GB/document_library/Scientific_guideline/2009/09/WC500003272.pdf⟩.
[24] C. Kilkenny, W. Browne, I.C. Cuthill, M. Emerson, D.G. Altman, Animal research: reporting in vivo experiments: the arrive guidelines, Br. J. Pharmacol. 160 (2010) 1577–1579, https://doi.org/10.1111/j.1476-5381.2010.00872.x.
[25] J.C. McGrath, E. Lilley, Implementing guidelines on reporting research using animals (arrive etc.): new requirements for publication in BJP, Br. J. Pharmacol. 172 (2015) 3189–3193, https://doi.org/10.1111/bph.12955.
[26] F. Maione, M. Piccolo, S. De Vita, M.G. Chini, C. Cristiano, C. De Caro, P. Lippiello, M.C. Miniaci, R. Santamaria, C. Irace, V. De Feo, A. Calignano, N. Mascolo, G. Bifulco, Down regulation of pro- inflammatory pathways by tanshinone IIA and cryptotanshinone in a non-genetic mouse model of Alzheimer's disease, Pharmacol. Res. 129 (2018) 482–490, https://doi.org/10.1016/j.phrs.2017.11.018.
[27] G. D'Agostino, R. Russo, C. Avagliano, C. Cristiano, R. Meli, A. Calignano, Palmitoylethanolamide Protects against the Amyloid-β25-35-induced learning and memory impairment in mice, an experimental model of Alzheimer disease, Neuropsychopharmacology 37 (2012) 784–1792, https://doi.org/10.1038/npp.2012.25.
[28] W. Blaine Stine, L. Jungbauer, C. Yu, M. Jo LaDu, Preparing synthetic A β in different aggregation states, Methods Mol. Biol. 670 (2011) 13–32, https://doi.org/10.1007/978-1-60761-744-0_2.
[29] F. Raucci, A.J. Iqbal, A. Saviano, P. Minosi, M. Piccolo, C. Irace, F. Caso, R. Scarpa, S. Pieretti, N. Mascolo, F. Maione, IL-17A neutralizing antibody regulates monosodium urate crystal-induced gouty inflammation, Pharmacol. Res. 147 (2019), 104351, https://doi.org/10.1016/j.phrs.2019.104351.
[30] S. Kim, D. Foong, M.S. Cooper, M.J. Seibel, H. Zhou, Comparison of blood sampling methods for plasma corticosterone measurements in mice associated with minimal stress-related artefacts, Steroids 135 (2018) 69–72, https://doi.org/10.1016/j.steroids.2018.03.004.
[31] M.J. Curtis, S. Alexander, G. Cirino, J.R. Docherty, C.H. George, M.A. Giembycz, A. Gilchrist, D. Hoyer, P.A. Insel, A.A. Izzo, A.J. Lawrence, D.J. MacEwan, L. D. Moon, S. Wonnacott, A.H. Weston, J.C. McGrath, Experimental design and analysis and their reporting II: updated and simplified guidance for authors and peer reviewers, Br. J. Pharmacol. 175 (2018) 987–993, https://doi.org/10.1111/bph.12856.
[32] S.P.H. Alexander, R.E. Roberts, B.R.S. Broughton, C.G. Sobey, C.H. George, S. C. Stanford, G. Cirino, J.R. Docherty, M.A. Giembycz, D. Hoyer, P.A. Insel, A. A. Izzo, Y. Ji, D.J. MacEwan, J. Mangum, S. Wonnacott, A. Ahluwalia, Goals and practicalities of immunoblotting and immunohistochemistry: a guide for submission to The British Journal of Pharmacology, Br. J. Pharmacol. 175 (2018) 407–411, https://doi.org/10.1111/bph.14112.
[33] C.H. George, S.C. Stanford, S. Alexander, G. Cirino, J.R. Docherty, M.A. Giembycz, D. Hoyer, P.A. Insel, A.A. Izzo, Y. Ji, D.J. MacEwan, C.G. Sobey, S. Wonnacott, A. Ahluwalia, Updating the guidelines for data transparency in the British Journal of Pharmacology - data sharing and the use of scatter plots instead of bar charts, Br. J. Pharmacol. 174 (2017) 2801–2804, https://doi.org/10.1111/bph.13925.
[34] E.A. Newcombe, J. Camats-Perna, M.L. Silva, N. Valmas, J. Huat, R. Medeiros, Inflammation: the link between comorbidities, genetics, and Alzheimer's disease, J. Neuroinflamm. 15 (2018) 276, https://doi.org/10.1186/s12974-018-1313-3.
[35] M. D'Amelio, S. Puglisi-Allegra, N. Mercuri, The role of dopaminergic midbrain in Alzheimer's disease: translating basic science into clinical practice, Pharmacol. Res. 30 (2018) 414–4119, https://doi.org/10.1016/j.phrs.2018.01.016.
[36] B.O.A. Botchway, M.K. Moore, F.O. Akinleyes, I.C. Iyer, M. Fang, Nutrition: review on the possible treatment for Alzheimer's disease, J. Alzheimers Dis. 61 (3) (2018) 867–883, https://doi.org/10.3233/JAD-170874.
[37] F. Pistollato, R.C. Iglesias, R. Ruiz, S. Aparicio, J. Crespo, L.D. Lopez, P.P. Manna, F. Giampieri, M. Battino, Nutritional patterns associated with the maintenance of neurocognitive functions and the risk of dementia and Alzheimer's disease: a focus on human studies, Pharmacol. Res. 131 (2018) 32–43, https://doi.org/10.1016/j.phrs.2018.03.012.
[38] S. Habtemariam, Natural products in Alzheimer's disease therapy: would old therapeutic approaches fix the broken promise of modern medicines? Molecules 24 (8) (2019) 1519, https://doi.org/10.3390/molecules24081519.
[39] R.E. Mrak, W.S. Griffinbc, The role of activated astrocytes and of the neurotrophic cytokine S100B in the pathogenesis of Alzheimer's disease, Neurobiol. Aging 22 (6) (2001) 915–922, https://doi.org/10.1016/s0197-4580(01)00293-7.
[40] M. Pekny, M. Nilsson, Astrocyte activation and reactive gliosis, Glia 50 (4) (2005) 427–434, https://doi.org/10.1002/glia.20207.
[41] S. Fuller, M. Steele, G. Münch, Activated astroglia during chronic inflammation in alzheimer's disease—do they neglect their neurosupportive roles? Mutat. Res. Fundam. Mol. Mech. 690 (2010) 40–49, https://doi.org/10.1016/j.mrfmmm.2009.08.016.
[42] L.J. Van Eldik, M.S. Wainwright, The Janus face of glial-derived S100B: beneficial and detrimental functions in the brain, Restor. Neurol. Neurosci. 3–4 (2003) 97–108.
[43] R.E. Mrak, W.S.T. Griffin, Glia and their cytokines in progression of neurodegeneration, Neurobiol. Aging 26 (2005) 349–354, https://doi.org/10.1016/j.neurobiolaging.2004.05.010.
[44] A.J. Vincent, R. Gasperini, L. Foa, D.H. Small, Astrocytes in alzheimer's disease: emerging roles in calcium dysregulation and synaptic plasticity, J. Alzheimer's Dis. 22 (3) (2010) 699–714, https://doi.org/10.3233/JAD-2010-101089.
[45] M.Q. Xia, B.T. Hyman, Chemokines/chemokine receptors in the central nervous system and Alzheimer's disease, J. Neurovirol. 5 (1999) 32–41, https://doi.org/10.3109/13550289909029743.
[46] K. Rostasy, C. Egles, A. Chauhan, M. Kneissl, P. Bahrani, C. Yiannoutsos, B. A. Navia, SDF-1α is expressed in astrocytes and neurons in the AIDS dementia complex: an in vivo and in vitro study, J. Neuropathol. Exp. Neurol. 62 (2003) 617–626, https://doi.org/10.1093/jnen/62.6.617.
[47] G. Azizi, N. Khannazer, A. Mirshafiey, The potential role of chemokines in Alzheimer's disease pathogenesis, Am. J. Alzheimer's. Dis. Dement. 29 (2014) 415–425, https://doi.org/10.1177/1533317513518651.
[48] D.G. Walker, L.F. Lue, T.M. Tang, C.H. Adler, J.N. Caviness, M.N. Sabbagh, T. G. Beach, Changes in CD200 and intercellular adhesion molecule-1 (ICAM-1) levels in brains of Lewy body disorder cases are associated with amounts of Alzheimer's pathology not α-synuclein pathology, Neurobiol. Aging 54 (2017) 175–186, https://doi.org/10.1016/j.neurobiolaging.2017.03.007.
[49] J. Emerit, M. Edeas, F. Bricaire, Neurodegenerative diseases and oxidative stress, Biomed. Pharmacother. 58 (1) (2004) 39–46, https://doi.org/10.1016/j.biopha.2003.11.004.
[50] E. Radi, P. Formichi, C. Battisti, A. Federico, Apoptosis and oxidative stress in neurodegenerative diseases, J. Alzheimers Dis. 42 (Suppl 3) (2014) S125–S152, https://doi.org/10.3233/JAD-132738.
[51] M.A. Smith, X. Zhu, M. Tabaton, G. Liu, D.W. McKeel Jr., M.L. Cohen, X. Wang, S. L. Siedlak, B.E. Dwyer, T. Hayashi, M. Nakamura, A. Nunomura, G. Perry, Increased iron and free radical generation in preclinical Alzheimer disease and mild cognitive impairment, J. Alzheimers Dis. 19 (2010) 363–372, https://doi.org/10.3233/JAD-2010-1239.
[52] S. Levi, D. Finazzi, Neurodegeneration with brain iron accumulation: update on pathogenic mechanisms, Front. Pharmacol. 5 (2014) 99, https://doi.org/10.3389/fphar.2014.00099.
[53] E. Mills, X.P. Dong, F. Wang, H. Xu, Mechanisms of brain iron transport: insight into neurodegeneration and CNS disorders, Future Med. Chem. 2 (1) (2010) 51–64, https://doi.org/10.4155/fmc.09.140.
[54] D.J.R. Lane, S. Ayton, A.I. Bush, Iron and Alzheimer's disease: an update on emerging mechanisms, J. Alzheimers Dis. 64 (s1) (2018) S379–S395, https://doi.org/10.3233/JAD-179944.
[55] M.A. Smith, P.L. Harris, L.M. Sayre, G. Perry, Iron accumulation in Alzheimer disease is a source of redox-generated free radicals, Proc. Natl. Acad. Sci. USA 94 (1997) 9866–9868, https://doi.org/10.1073/pnas.94.18.98.
[56] Z.M. Qian, P.L. Tang, Mechanisms of iron uptake by mammalian cells, Biochim. Biophys. Acta 1269 (1995) 205–214, https://doi.org/10.1016/0167-4889(95)00098-X.
[57] K. Zou, J.S. Gong, K. Yanagisawa, M. Michikawa, A novel function of monomeric amyloid beta-protein serving as an antioxidant molecule against metal-induced oxidative damage, J. Neurosci. 22 (2002) 4833–4841, https://doi.org/10.1523/JNEUROSCI.22-12-04833.2002.